

Fluid inclusions as tectonothermobarometers: Relation between pressure-temperature history and reequilibration morphology during crustal thickening

M. O. Vityk
R. J. Bodnar
C. S. Schmidt

Fluids Research Laboratory, Department of Geological Sciences,
Virginia Polytechnic Institute and State University,
Blacksburg, Virginia 24061

ABSTRACT

Results of experimental reequilibration studies of natural primary aqueous inclusions in quartz under conditions of hydrostatic compressive loading at 1, 2, 3, 4, and 5 kbar and 500 °C indicate that the intensity of reequilibration features is inversely proportional to inclusion volume. The smallest inclusions show the first evidence of reequilibration (dissolution of inclusion walls) after ~1.8 kbar of effective pressure. For effective pressures less than ~3.8 kbar, decrepitation of inclusions is probably controlled by the corrosive action of water on the inclusion walls. At higher effective pressures, decrepitation is related to high compressive stress and is less dependent on fluid interaction with the inclusion walls. The observed correlation between inclusion size, intensity of reequilibration features, and amount of loading, combined with paragenetic and microthermometric data for the inclusions, may be used to determine the pressure-temperature history of the inclusions and their host rocks.

INTRODUCTION

Fluid inclusions have been used for decades to determine the pressure-temperature-composition (*PTX*) conditions associated with various geologic processes. The validity of such determinations is based on the assumptions that (1) the inclusion traps a single, homogeneous fluid, (2) nothing is added to or lost from the inclusion after trapping and, (3) the inclusion volume remains constant. For many inclusions these assumptions hold, and the inclusions may be used to infer the formation conditions. In some environments, however, there is clear evidence that one or more of these assumptions is not valid, precluding the use of the inclusions to define the *PTX* conditions of formation.

If either or both of assumptions 2 and 3 above are violated, the fluid inclusion is said to have reequilibrated. Inclusions may reequilibrate if the *P-T* path followed by the host mineral differs from the isochore corresponding to the inclusion formation conditions. These paths may, in turn, be divided into those that result in the internal pressure in the inclusion exceeding the confining pressure (internal overpressure) and those resulting in internal pressures lower than the confining pressure (internal underpressure). The difference between the confining and internal pressures is referred to as the effective pressure ($P_{\text{eff}} = P_{\text{confining}} - P_{\text{internal}}$). Reequilibration may involve various mechanisms, and each mechanism produces characteristic morphological features on the walls and/or in the host mineral surrounding the parent inclusion. Moreover, the intensities of the textural features produced are now known to vary significantly depending upon the *P-T* conditions of reequilibration. As such, fluid-inclusion reequilibration textures, combined with standard microthermometric data obtained from the inclusions, may be used to infer the tectonic and thermobaric evolution of the host rocks (e.g., Boullier et al., 1991; Vityk et al., 1993).

Two types of fluid-inclusion reequilibration textures are de-

scribed in the literature: "explosion" textures formed under conditions of internal overpressure, and "implosion" textures formed under conditions of internal underpressure. Recent experiments with synthetic fluid inclusions (Sterner and Bodnar, 1989) show that textures produced under conditions of internal overpressure do indeed differ from those produced under conditions of internal underpressure. However, the factors (*P-T* history, inclusion size, fluid composition, etc.) that control the type and intensity of the different textures have not been thoroughly investigated.

Experimental studies conducted at 1 atm indicate that large fluid inclusions tend to decrepitate at lower effective pressure than smaller inclusions (e.g., Bodnar et al., 1989). A similar correlation has also been noted for naturally decrepitated or "exploded" inclusions (e.g., Voznyak and Kalyuzhnyi, 1976; Hurai and Horn, 1992). The observed size dependence of decrepitation under conditions of internal overpressure is explained by stress concentration induced by flaws that scale with inclusion size (Wanamaker et al., 1990). Following this line of reasoning, the same positive relation between inclusion size and intensity of reequilibration is to be expected under conditions of internal underpressure. However, the opposite relation was recently noted by Hurai and Horn (1992), who suggested that a negative correlation between inclusion size and intensity of reequilibration features is indicative of inclusion implosion. This observation has profound implications for reconstructing the *P-T* history of the inclusions and their host rocks. If it is true that large inclusions reequilibrate most easily (lower effective pressure) under conditions of internal overpressure, and that the smallest inclusions reequilibrate most easily under conditions of internal underpressure, simple petrographic analysis of inclusion reequilibration features in a given sample provides a very effective means of determining whether the *P-T* path followed by the sample resulted in over- or underpressures in the inclusions.

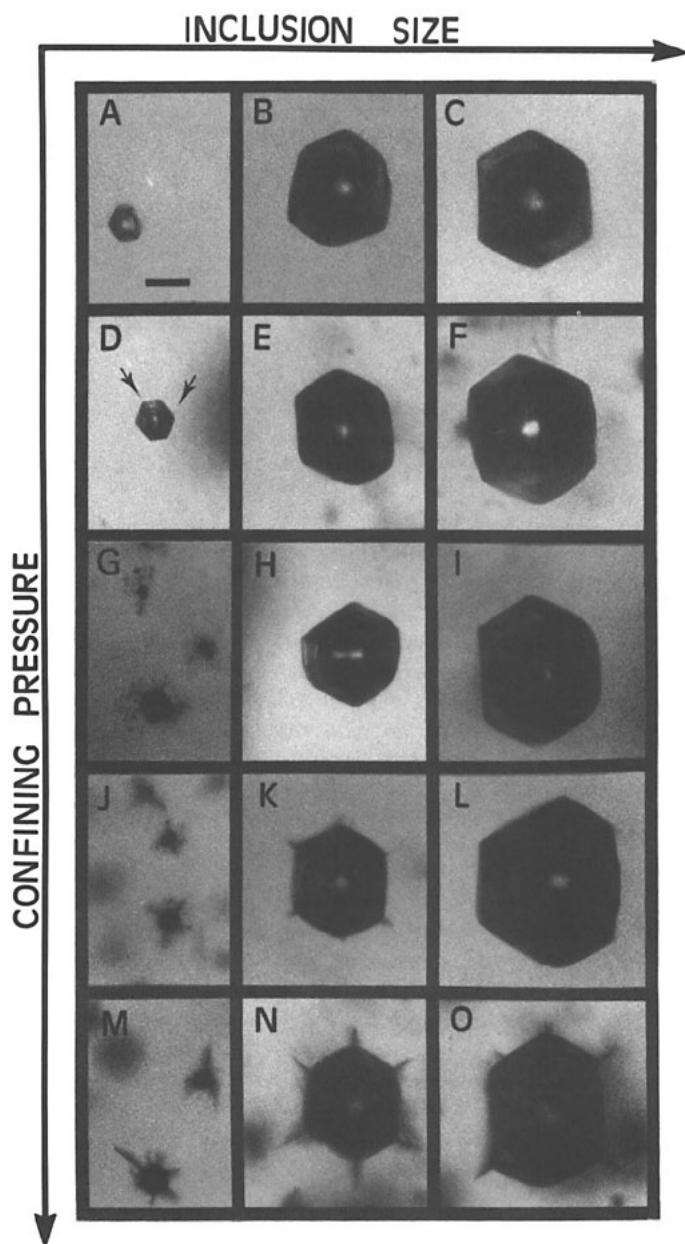


Figure 1. Photomicrographs showing reequilibration features for fluid inclusions of different size (volume) reequilibrated at 500 °C and 1 (A–C), 2 (D–F), 3 (G–I), 4 (J–L), and 5 (M–O) kbar for 7 d. All inclusions had approximately same internal pressure at 500 °C; thus, increasing confining pressure represents increased loading or simulated crustal thickening. Arrows in D point to dissolution pits originating at corners of negative-crystal-shaped inclusion. Scale bar represents 30 μm .

We have conducted experiments to determine the relation between inclusion size and intensity of reequilibration features under conditions of compressive loading. Natural fluid inclusions were used because questions remain concerning the applicability of results from studies of synthetic fluid inclusions to those from natural inclusions.

EXPERIMENTAL DETAILS

A quartz crystal about $6 \times 4 \times 2.5$ cm collected from a miarolitic pegmatite within the Bayanovoo Mesozoic biotite granite massif in central Mongolia was used in the experiments. The sample was cut parallel to the *c* axis to obtain the maximum size of the polished

plate for inclusion petrography. The majority of the inclusions are of primary origin, as evidenced by their localization along obvious growth zones, and most display a negative-crystal shape. These inclusions were trapped in the two-phase field as evidenced by the presence of liquid-rich, halite-bearing inclusions and vapor-rich inclusions in the same growth zone.

The three types of inclusions observed were (1) vapor-rich, two-phase inclusions, (2) liquid-rich, halite-bearing inclusions, and (3) mixed inclusions that trapped varying amounts of each of the end-member phases. The vapor-rich inclusions were used for the reequilibration study because of their low densities and relatively flat isochores, resulting in low internal pressures at the experimental temperature of 500 °C. Inclusion size varied from 5 to 500 μm in diameter. Salinity ranged from 2 to 6 wt% NaCl equivalent. The apparent homogenization temperature (T_h) of these inclusions was 350–420 °C. The minimum T_h of the coexisting liquid-rich, halite-bearing inclusions is 350 °C. The corresponding equilibrium vapor pressure at 350 °C is 0.12 kbar, assuming that these inclusions can be adequately described by using properties of the system H_2O -NaCl. The calculated low pressure is consistent with the shallow setting of this and many other anorogenic Mesozoic granites in eastern and central Mongolia. At the temperature of the experiments (500 °C), the internal pressure of the vapor-rich inclusions is estimated to be 200 ± 100 bar.

Five small (3×3 mm) polished sections, each containing vapor-rich fluid inclusions from 5 to 200 μm in diameter, were selected for reequilibration experiments. To evaluate the effect of inclusion volume on the reequilibration behavior, inclusions were divided into three size groups: small (diameter ≤ 40 μm), medium (diameter 40–90 μm), and large (diameter > 90 μm). Selected fluid inclusions were reequilibrated at 500 °C and 1, 2, 3, 4, and 5 kbar for 7 d in cold-seal pressure vessels using techniques described by Sterner and Bodnar (1989).

RESULTS

Morphological features of reequilibrated inclusions and the relation between inclusion size and intensity of reequilibration features are documented by a series of photomicrographs (Fig. 1). Inclusions subjected to 0.8 kbar of effective pressure (1 kbar experiment) showed no textural changes that would suggest that reequilibration occurred during the experiment (Fig. 1, A–C).

Small inclusions reequilibrated at 2 kbar ($P_{\text{eff}} = 1.8$ kbar) showed dissolution and recrystallization to produce an irregular scalloped texture on the inclusion-wall surface (Fig. 1D). The most intense dissolution was observed at the terminations of the negative crystal (arrows, Fig. 1D). No visible fractures were associated with any of the inclusions. Medium and large inclusions showed no evidence of reequilibration at these conditions (Fig. 1, E and F).

Small inclusions reequilibrated at 3 kbar ($P_{\text{eff}} = 2.8$ kbar) showed intense brittle deformation (Fig. 1G), and a halo of small inclusions commonly surrounds the parent inclusion in all directions. Medium and large inclusions (Fig. 1, H and I) showed no evidence of reequilibration at these conditions.

Small inclusions reequilibrated at 4 kbar ($P_{\text{eff}} = 3.8$ kbar) displayed intense dissolution-recrystallization of the inclusion walls, resulting in a distinct change in the inclusion shape (Fig. 1J). Fractures were better developed compared to smaller amounts of loading, and the length of fractures was usually less than or equal to the inclusion diameter. Medium-sized inclusions showed short, well-developed fractures originating at crystal terminations of the negative crystal (Fig. 1K), but large inclusions showed no evidence of reequilibration (Fig. 1L).

All of the inclusions that reequilibrated at 5 kbar ($P_{\text{eff}} = 4.8$

kbar; Fig. 1, M–O) decrepitated to produce a starlike texture. Dissolution of the inclusion walls, producing scalloped textures, was common, and the most intense dissolution features were observed for small inclusions. The lengths of fractures produced in the 5 kbar experiment were generally longer than those associated with the 4 kbar experiment. Note, however, that the crack length is inversely related to inclusion size. Cracks associated with smaller inclusions tended to propagate farther into the surrounding host crystal as compared to those associated with larger inclusions.

DISCUSSION

It is a well-known, although perhaps counterintuitive, fact that the nucleation, growth, and interaction of fractures can be a dominant mechanism in the short-term compressive deformation of brittle rocks (Paterson, 1978). Cracks grow because the stress in the region surrounding the fracture is sufficient to cause the tensile stress intensity factor at the crack tip to equal the critical value. In some cases, fractures can propagate under less than critical conditions as, for example, in the presence of chemically active species such as water. Examples of processes in which “subcritical crack growth” may be important include stress corrosion, diffusion, dissolution, ion exchange, and microplasticity (e.g., Atkinson, 1984).

The reequilibration behavior of aqueous inclusions used in this study is interpreted in the context of subcritical crack formation. Effective pressure, chemical activity of the stress corrosion agent (which is in turn a function of pressure, temperature, and fluid composition), and inclusion shape and volume are the important factors in subcritical crack growth in our experiments. All of the inclusions used have similar salinities (~5 wt% NaCl equivalent), densities, and geometries (negative-crystal shape) but have variable sizes. Each size group showed different morphological features as a result of reequilibration, and the intensity of reequilibration features was found to be inversely proportional to the inclusion size.

Small inclusions reequilibrated at 2 kbar and 500 °C display dissolution features that are best developed as dissolution pits at the corners of the fluid inclusion (Fig. 1D). At the same time, no dissolution features were associated with medium and large fluid inclusions at these conditions. This behavior is described by a modified form of the Kelvin equation, which relates the solubility to the size of the dissolving phase and its surface free energy (Adamson, 1982). The modified Kelvin equation describes the relation between a negative crystal (inclusion cavity) in a solid and the fluid according to

$$S(r)/S_0 = \exp[2GV/RT(-r)], \quad (1)$$

where $S(r)$ is the solubility (in a solid) of fluid in an inclusion with radius r , S_0 is the bulk solubility, G is the Gibbs free energy of the solid-solution interface, V is molar volume of the solid, R is the gas constant, and T is the absolute temperature. In this case a minus sign is used in front of r to indicate the negative curvature for the radius of the negative crystal.

According to equation 1, fluid will “dissolve” into the solid in proportions inversely related to the inclusion radius. Although the solubility of H₂O in quartz at these P - T conditions is small (a few hundred ppm), sufficient water is present to generate 10⁶ to 10⁷ fluid inclusions/cm³ of quartz as a result of exsolution during cooling from 700 °C and 7 kbar (Spear and Selverstone, 1983). It is predicted that the fracture strength of the mineral surrounding a small inclusion will be reduced considerably, relative to a larger inclusion, as a result of water-induced corrosion. The resulting dissolution pits at the terminations of negative crystals (Fig. 1D) are potential nucleation sites for further cracking. At higher stresses, adsorption of water at the crack tip will increase the velocity of crack propagation (Atkinson,

1984). Thus, after 3 kbar of loading, dissolution pits are replaced by small thin cracks decorated by secondary inclusions (Fig. 1G). As stress (pressure) increases (4 and 5 kbar experiments) the intensity (length and thickness) of cracks for small inclusions increases proportionally (Fig. 1, J and M). The first evidence of dissolution and brittle deformation of the inclusion walls for the medium-sized inclusions was observed after the 4 kbar experiment (Fig. 1K). Finally, after the 5 kbar experiment, all fluid inclusions had decrepitated (Fig. 1, M–O). The intensity of the decrepitation features for small inclusions (intense dissolution) is higher than that for large inclusions (minor or no dissolution features observed). At ~4.8 kbar of P_{eff} the decrepitation of fluid inclusions is controlled mainly by mechanical rupture and appears to be less sensitive to fluid chemical action.

Fluid composition is an important factor in fracture nucleation and propagation behavior. The importance of fluid composition in fluid-inclusion reequilibration is evidenced by results of a reequilibration experiment using natural methane fluid inclusions that formed at 230 °C and 0.54 kbar (Kalyuzhnyi, 1993). The inclusions are vapor-rich and range in size from ~10 to 60 μm. Although no water was observed in these inclusions, some small amounts of water could be present as a thin film around the inclusion walls. The inclusions were subjected to compressive loading at 500 °C and 5 kbar for 7 d at an effective pressure of 4.1 kbar. No reequilibration textures were associated with any of the methane-bearing inclusions after the experiment. Conversely, aqueous inclusions of similar size and geometry described previously showed dissolution of the inclusion walls at ~1.8 kbar of effective pressure (Fig. 1D), and all of the aqueous inclusions decrepitated when P_{eff} reached 4.8 kbar (Fig. 1, M–O). Thus, by using results from the aqueous inclusions for comparison, the small and medium-sized methane inclusions should have shown obvious reequilibration textures after the experiment. We attribute the absence of these features to the fact that the methane inclusions contain little or no water, which would promote subcritical crack growth.

APPLICATIONS

How can the information obtained in this study be used to help decipher the tectonic and thermobaric history of a geologic sample? In fluid-inclusion studies, we measure a homogenization temperature, which allows us to construct an isochore for the inclusion. The isochore then represents a locus of pressure-temperature points, and the inclusion must have intersected this locus of points at some time during its evolution. The question, then, is whether this locus of points represents the original formation conditions, or some pressure-temperature condition to which the inclusion has reequilibrated following entrapment. If the latter, we would also like to know the relation between the new “reequilibrated isochore” and the original isochore representing inclusion formation.

Suppose a sample contains aqueous inclusions with a homogenization temperature (T_h) and isochore (reequilibration isochore) as shown in Figure 2. From the measured homogenization temperature alone we have no way of knowing whether the isochore represents original formation conditions or some later reequilibration condition. However, if petrographic examination of the inclusions reveals intense deformation of the smallest inclusions, with scalloped-textured walls and halos of smaller inclusions around the parent inclusion (Fig. 1G), but no evidence of reequilibration of larger inclusions, the results of this study would suggest that the sample was subjected to ~3 kbar of loading following formation. Thus, the isochore for the aqueous inclusions represents the reequilibration conditions (Fig. 2), and the original formation conditions are constrained to lie along a locus of P - T points that are 3 kbar below the reequilibration isochore (e.g., points A1, B1, C1, and D1, Fig. 2). If we

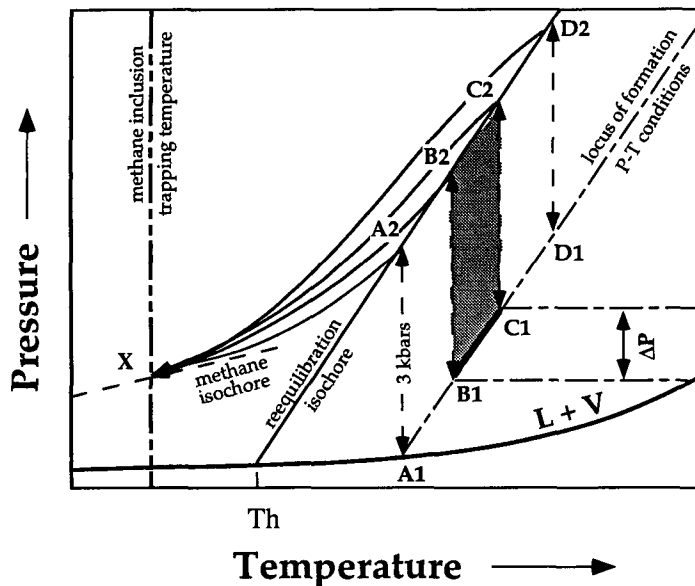


Figure 2. Schematic representation of application of data from reequilibrated fluid inclusions to constrain pressure-temperature path. T_h represents homogenization temperature of reequilibrated inclusions along liquid-vapor curve (L+V) and reequilibration isochore represents isochore for these inclusions. Textural evidence suggests that these inclusions have undergone 3 kbar of loading, constraining locus of formation P - T conditions to lie along line A1-D1. Original formation pressure range (ΔP) imposed by an independent geobarometer limits starting point of uplift path to part of line B1-C1 (heavy line). Low-temperature part of the path is defined by intersection of a methane inclusion isochore with its trapping temperature. P - T path defined by combined microthermometric and textural information is constrained to pass through shaded area.

assume that the reequilibration textures shown by the inclusions reflect the maximum internal pressure encountered by the inclusions (as is expected), and if we assume that the inclusions do not undergo retrograde reequilibration as the internal pressure decreases from the maximum of 3 kbar (as is also likely), then the path followed by the inclusions must originate along the line A1-D1 and follow an increasing pressure path to intersect the reequilibration isochore (A2-D2), and then follow a decreasing pressure path during uplift. So, by combining paragenetic and microthermometric data for the inclusions with textural information that defines the magnitude of loading, we are able to show that the sample that initially formed at high temperatures and moderate pressures subsequently was involved in a crustal thickening event that raised the confining pressure. If we are able to constrain the formation pressure of the inclusions using a mineralogical geobarometer (ΔP , Fig. 2), then the inclusion origin and path are further constrained, as indicated by the shaded area in Figure 2. Finally, the later, low-temperature part of the path may be constrained by isochores representing later inclusions, as shown by the methane isochore (Fig. 2).

Our results suggest that fluid-inclusion reequilibration textures produced under conditions of loading are fundamentally and recognizably different from those produced under conditions of internal overpressure. Specifically, we have documented experimentally that small inclusions reequilibrate at lower effective pressures than larger inclusions during loading or crustal thickening. Conversely, the largest inclusions reequilibrate first if the effective pressure ($P_{\text{eff}} = P_{\text{confining}} - P_{\text{internal}}$) is negative (Bodnar et al, 1989). Thus, documentation of which inclusions (i.e., the smallest or the largest) show the most intense reequilibration features can provide a significant constraint on tectonic history. It is important to remember that

our reequilibration experiments were conducted over a period of 7 d with instantaneous loading, and the effect of time and strain rate on the intensity and morphology of reequilibration characteristics has not been considered. This introduces the possibility that the size effect may be eliminated over geologic time and that all inclusions, regardless of size, would reequilibrate to the same extent. However, reports of natural inclusions showing both negative and positive correlations between size and intensity in samples from various geologic environments suggest that these reequilibration textures can be preserved over geologic time (Hurrai and Horn, 1992; Vityk et al., 1993). These data suggest that morphological characteristics of reequilibrated inclusions, combined with paragenetic and microthermometric data from the same inclusions, can be used to decipher the tectonic history of geologically complex terranes.

ACKNOWLEDGMENTS

We thank J. D. Rimstidt, M. Hochella, E. Roedder, D. P. Hasselman, and R. Reynolds for helpful discussions and constructive comments. Reviews of an earlier version of this manuscript by Jane Selverstone and an anonymous reviewer have helped clarify many aspects of this study.

REFERENCES CITED

- Adamson, A. W., 1982, *Physical chemistry of surfaces*: New York, John Wiley & Sons, 664 p.
- Atkinson, B. K., 1984, Subcritical crack growth in geological material: *Journal of Geophysical Research*, v. 89, p. 4077-4114.
- Bodnar, R. J., Binns, P. R., and Hall, D. L., 1989, Synthetic fluid inclusions. IV. Quantitative evaluation of the decrepitation behavior of fluid inclusion in quartz at one atmosphere confining pressure: *Journal of Metamorphic Geology*, v. 7, p. 229-242.
- Boullier, A. M., France-Lanord, C., Dubessy, J., Adamy J., and Champeinois, M., 1991, Linked fluid and tectonic evolution in the High Himalayan Mountains (Nepal): *Contributions to Mineralogy and Petrology*, v. 107, p. 358-372.
- Hurrai, V., and Horn, E., 1992, A boundary layer-induced immiscibility in naturally reequilibrated H_2O - CO_2 - $NaCl$ inclusions from metamorphic quartz (Western Carpathians, Czechoslovakia): *Contributions to Mineralogy and Petrology*, v. 112, p. 414-427.
- Kalyuzhnyi, V. A., 1993, The peculiarities of the evolution of hydrothermal fluids H_2O - CH_4 - C_nH_m as a medium of the rock-crystal ("Marmarosh Diamonds") crystallization from the Ukrainian Carpathians (abs.): *Archiwum Mineralogiczne*, v. 49, p. 109-110.
- Paterson, M. S., 1978, *Experimental rock deformation: The brittle field*: New York, Springer-Verlag, 254 p.
- Spear, F. S., and Selverstone, J., 1983, Water exsolution from quartz: Implication for the generation of retrograde metamorphic fluids: *Geology*, v. 11, p. 82-85.
- Sterner, S. M., and Bodnar, R. J., 1989, Synthetic fluid inclusions. VII. Reequilibration of fluid inclusions in quartz during laboratory simulated metamorphic burial and uplift: *Journal of Metamorphic Geology*, v. 7, p. 243-260.
- Vityk, M. O., Anderson, A. J., Bodnar, R. J., and Dudok, I., 1993, Reequilibration characteristics of fluid inclusions in "Marmarosh Diamonds": Evidence for tectonic history of Ukrainian Carpathians? (abs.): *Archiwum Mineralogiczne*, v. 49, p. 235-236.
- Voznyak, D. K., and Kalyuzhnyi, V. A., 1976, Utilization of decrepitated inclusions for reconstruction of PT conditions of mineral formation (an example of pegmatitic quartz from Volyn): *Mineralogicheskyy Sbornik*, v. 30, p. 31-40 (in Russian).
- Wanamaker, B. J., Wong, T.-F., and Evans, B., 1990, Decrepitation and crack healing of fluid inclusions in San Carlos olivine: *Journal of Geophysical Research*, v. 95, p. 15,623-15,641.

Manuscript received February 7, 1994
 Revised manuscript received May 5, 1994
 Manuscript accepted May 10, 1994